Quantitative Selected Ion Flow Tube Mass Spectrometry: The Influence of Ionic Diffusion and Mass Discrimination

Patrik Španěl
V. Čermák Laboratory, J. Heyrovský Institute of Physical Chemistry, Academy of Sciences of the Czech Republic, Dolejškova, Prague, Czech Republic

David Smith
Centre for Science and Technology in Medicine, School of Postgraduate Medicine, Keele University, Hartshill, Stoke-on-Trent, UK

Selected ion flow tube mass spectrometry, (SIFT-MS), involves the partial conversion of mass-selected precursor ions to product ions in their reactions with the trace gases in an air sample that is introduced into helium carrier gas in a flow tube. The precursor and product ions are then detected and counted by a downstream quadrupole mass spectrometer. Quantification of particular trace gases is thus achieved from the ratio of the total count rate of the product ions to that for the precursor ions. However, it is important to appreciate that in this ion chemistry the light precursor ions (usually H_3O^+ ions) are invariably converted to heavier product ions. Hence, the product ions diffuse to the flow tube walls more slowly and thus they are more efficiently transported to the downstream mass spectrometer sampling orifice. This phenomenon we refer to as diffusion enhancement. Further, it is a well-known fact that discrimination can occur against ions of large mass-to-charge ratio, (m/z), in quadrupole mass spectrometers. If not accounted for, diffusion enhancement usually results in erroneously high trace gas concentrations and mass discrimination results in erroneously low concentrations. In this experimental investigation, we show how both these counteracting effects can be accounted for to increase the accuracy of SIFT-MS quantification. This is achieved by relating the currents of ions of various m/z that arrive at the downstream mass spectrometer sampling orifice disc to their count rates at the ion detector after mass analysis. Thus, both diffusion enhancement and mass discrimination are parameterized as a function of m/z and these are combined to provide an overall discrimination factor for the particular analytical instrument. (J Am Soc Mass Spectrom 2001, 12, 863–872) © 2001 American Society for Mass Spectrometry

During the last five years, we have exploited the selected ion flow tube (SIFT) as a new analytical technique for the direct quantification of trace gases in atmospheric air and exhaled breath down to the parts per billion level, avoiding the need to first collect and pre-concentrate the air/breath samples [1–3]. This technique is now called selected ion flow tube mass spectrometry, (SIFT-MS) [4, 5]. It exploits chemical ionization [6] (under truly thermalized conditions) along a flow tube during a well-defined time period of the trace gases in the sample using judiciously chosen positive ions. A major motivation for this development was the need for on-line quantification of trace gases in human breath for clinical diagnosis and therapeutic monitoring [7]. We are beginning to make significant headway in this work [3] and are demonstrating the great potential of SIFT-MS as a tool for non-invasive physiological monitoring [8, 9]. Other valuable applications are now emerging in agriculture and animal husbandry [10, 11], environmental research, and food technology [4]. In common with most new techniques developments, the understanding of the details of operation has improved with time, and the demands for greater accuracy and for proper validation [12, 13] of the technique have grown, especially when it is used in medicine. In the initial stages of SIFT-MS development, a factor of two in the accuracy of real time (on-line) quantification of trace gases in air/breath samples was acceptable, which can usually allow recognition of some diseased compared to healthy states by breath analysis alone. Now it has become increasingly desirable to tighten up these analyses and a step in this direction was taken by accounting for the influence on the analyses of the relatively large amounts of water

Published online May 10, 2001

Address reprint requests to Dr. D. Smith, Centre for Science and Technology in Medicine, School of Post-Graduate Medicine, Keele University, Thornburrow Drive, Hartshill, Stoke-on-Trent, ST4 7QB, UK. E-mail: d.smith@bemp.keele.ac.uk

1044-0305/01/$20.00
PII S1044-0305(01)00253-7

Received January 22, 2001
Revised February 16, 2001
Accepted February 16, 2001

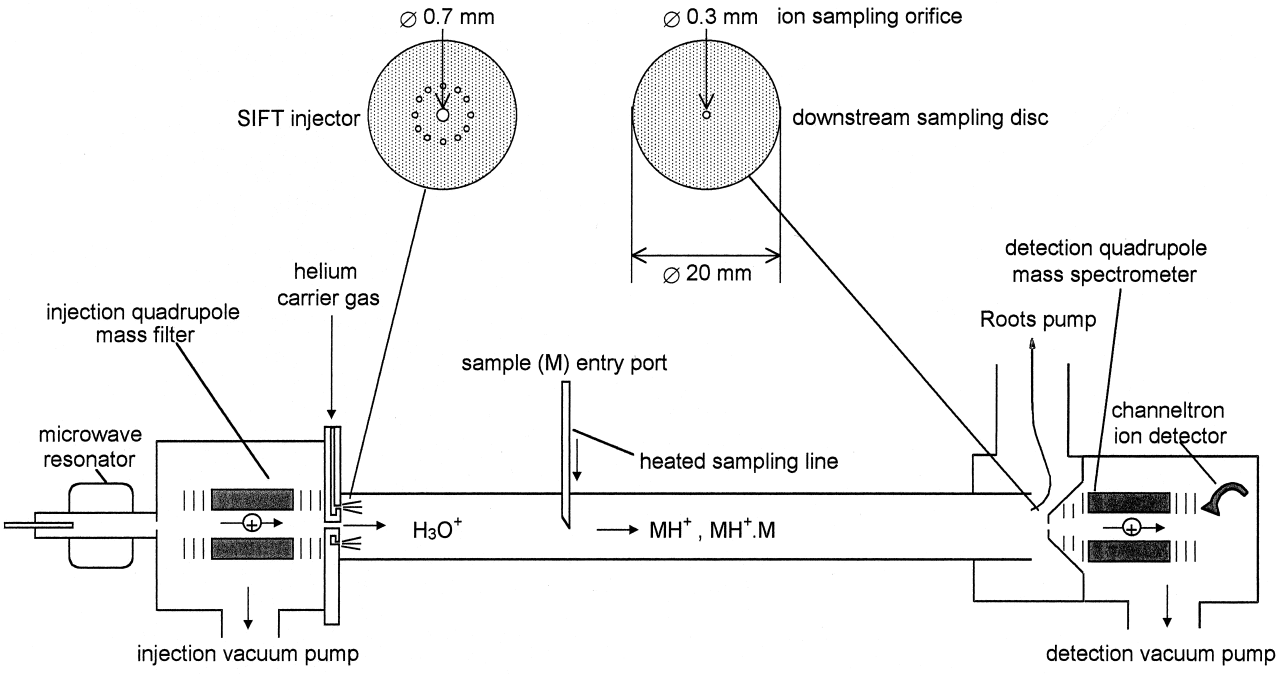

Figure 1. A schematic diagram of the TSIFT apparatus, showing its essential components. Detailed views of the SIFT injector and of the downstream sampling disc are also shown. See the text for further descriptions and references.

vapour that are present in moist air and breath samples [14]. For greater accuracy in quantification of trace gases, it is important to understand in more detail the physical principles involved in SIFT-MS, especially the ionic diffusion phenomena involved and the behavior of the analytical quadrupole mass spectrometer/ion sampling system with regard to mass discrimination. The results reported in this paper might also be relevant to other analyses that exploit chemical ionization mass spectrometry and flow tubes such as those used for atmospheric research [15, 16] and environmental measurements [17].

Selected Ion Flow Tube Mass Spectrometry

The SIFT-MS technique utilizes chemical ionization in a flow tube (Smith and Španěl, 1996 a, b; Španěl and Smith, 1996). Precursor ions of a given mass-to-charge ratio (selected by an upstream quadrupole mass filter) are injected into fast flowing helium carrier gas, which is introduced at near sonic speed via the 12 small holes as depicted in Figure 1. In this way, the Venturi effect is exploited and the back flow of helium into the injection mass filter is greatly reduced. This is the essence of the SIFT injector that has been described in detail in previous papers [18]. The precursor ions react during a defined reaction time with the trace gases in a sample of air, breath or liquid headspace, which is introduced into the carrier gas at a known flow rate, and produce characteristic product ions. A downstream (analytical) quadrupole mass spectrometer is used detect and count the precursor and product ions. The resultant mass spectrum (over a predetermined mass range) is acquired by an on-line computer which immediately identifies and quantifies the trace gases in the sample (see below) [1–3]. The precursor ions must not react at a significant rate with the major gases in air and breath (N_2, O_2, H_2O, CO_2 and Ar) but must react rapidly with the trace gases in the samples. H_3O^+ precursor ions are used to detect and quantify most organic vapours; they transfer their protons to the different trace gases, M, in the sample producing MH^+ ions. A fraction of the product MH^+ ions react with the water molecules to form their monohydrate, $MH^+ \cdot H_2O$, and sometimes their dihydrate, $MH^+ \cdot (H_2O)_2$. These hydrated ions are included in the product ion count for accurate quantification of the individual trace gases in the headspace gas [14]. Both NO^+ and O_2^+ ions are also routinely used as precursor ions [1–3]. Perhaps the most important advantage of SIFT-MS over other analytical techniques involving chemical ionization is that each of these three precursor ions can be selected at the flick of a switch on the upstream quadrupole mass filter controller. Essential for this SIFT-MS analytical method is the kinetics database of the reactions of H_3O^+, NO^+ and O_2^+ constructed from detailed studies of the reactions of these ions with a wide variety of compounds [19–28]. This database provides the rate coefficients, k, and the ion products for the reactions of the precursor ions with the trace gas molecules.

Quantitative Analysis Using the Kinetics of Ion-Molecule Reactions

The simple analytical procedure [2, 14] requires only a measurement of the precursor ion count rates (for

example [H_3O^+]) at the downstream mass spectrometer/detection system and the count rates [MH^+] of the product ions of the reaction of the precursor ions with those trace gas molecules present at a number density [M]. When [MH^+] $\ll$ [H_3O^+], the simple kinetics of the reactions show that the required [M] in the sample of air/breath is given by:

$$[M] = \frac{1}{t_r} \frac{[MH^+]}{k[H_3O^+]} \quad (1)$$

The reaction time t_r is determined from the flow velocity of the ions and the length of the flow tube, l, over which the reactions occur. The ion flow velocity is determined from a measurement of the carrier gas flow velocity as calculated from its flow rate and its pressure in the flow tube [2, 18]. This simple analysis has been discussed in depth in our previous papers [1, 2, 14]. Another strength of this analytical method is that quantification depends on the measurement of ion count rate ratios and not on absolute count rates of product ions that naturally follow drifts in the precursor ion intensities.

The exploratory experiments on SIFT-MS were carried out with our large laboratory SIFT (that utilizes a large Roots pump and a large analytical quadrupole mass spectrometer). This laboratory SIFT was primarily developed for the determination of the rate coefficients for ion-molecule reactions at thermal energies with specific reference to reactions that occur in the terrestrial atmosphere and in interstellar clouds [18, 29]. We validated the SIFT-MS analytical method with this large SIFT by creating standard mixtures using the syringe injection method [30] and permeation tube method [13]. These validations showed that trace gas concentration could be quantified in dry air to better than 10% [12, 13]. Later refinements of the analytical procedure have accounted for the influence on the ion chemistry of the large amounts of water vapor present in humid air and breath [7]. This has been dealt with in a very recent paper [14].

Differential Diffusion and Mass Discrimination

The inadequacy of both the simple (eq 1) and the refined analytical procedures (reported in ref. [14]) is that they ignore the occurrence of two potentially important phenomena. These are as follows.

1. **Differential diffusion** of precursor and product ions along the flow tube. This tends to enhance the currents of the (usually) heavier product ions arriving at the pinhole orifice through which the ions enter the downstream mass spectrometer detection system (Figure 1). If not accounted for, this will falsely enhance the count rates of the product ions and leads to an erroneously high [M]. We call this phenomenon diffusion enhancement and later describe its magnitude for product ions by a coefficient De.
2. **Mass discrimination** against the heavier ions in the analytical quadrupole mass spectrometer, a general feature of most quadrupole mass spectrometers [31]. This is especially sensitive to the resolution setting of the quadrupole and is somewhat dependent on the energy of the ions, E_i, in the analyzing field. We must also include under this heading the possible uneven sampling of the different mass ions from the helium carrier gas into the analytical mass spectrometer and the differential detection efficiencies of the channeltron ion multiplier that is used as the detector/amplifier in these instruments (Figure 1). We can combine the effects of these phenomena into one and describe a coefficient M_r that indicates the magnitude of discrimination against the (heavier) product ions compared to discrimination against the (usually lighter) precursor ions.

Clearly, diffusion enhancement of the product ions (by 1) is counteracted by mass discrimination (by 2). In the validations referred to above for the large laboratory SIFT, it turns out that because diffusion losses of ions were small along the flow tube (large diameter of 8 cm, and a larger carrier gas flow rate), differential diffusion enhancement of the heavier product ions was correspondingly small. Also, the large, high quality analytical quadrupole has only a relatively small discrimination towards the larger mass ions, at least for m/z values below 100. Therefore, these two counteracting effects mostly cancelled out and hence quantification of the trace gases in dry air samples was good over the ion mass range explored [8, 9, 32].

The great promise of this new analytical technique demanded the design and construction of a smaller, transportable SIFT apparatus in order to avoid undesirable bag sampling of breath and the time-consuming transport of bag samples to the immobile, large SIFT apparatus (which inevitably resulted in partial loss of breath metabolites). We have thus designed and constructed a transportable selected ion flow tube (TSIFT) instrument, in order to perform on-line SIFT-MS breath analyses in the hospital environment. The compromises that had to be made were the use of a smaller flow tube, a smaller Roots pump, and a smaller, more compact analytical quadrupole system. Our experiments with this TSIFT have shown those effects 1 and 2 above are more pronounced and must be accounted for in the analytical procedure. It has thus been necessary to consider more carefully the appropriate flow dynamics, reaction kinetics, and diffusion in these systems to study and account for mass discrimination and to properly quantify these phenomena. Of these, differential diffusion can, in principle, be understood and accounted for by suitable treatment of the flow dynamics and by the adoption of appropriate diffusion coefficients for ions of different mass, as we will show. It can also be assessed experimentally by measuring relative

currents of ions of varying masses arriving at the entrance to the downstream analytical mass spectrometer. Mass discrimination in the mass spectrometer cannot easily be treated theoretically, since this depends on the set-up of the particular analytical mass spectrometer. So, this is properly assessed and accounted for by an experimental investigation.

The purpose of this paper is to describe how these two phenomena separately influence the ion count rates in a TSIFT instrument and how they can be properly accounted for to provide more accurate quantification of trace gases in air/breath samples using the SIFT-MS technique. We now describe the appropriate experiments we have carried out using the TSIFT and the results obtained, which allow the magnitudes of diffusion enhancement (D_e) across the ionic mass range and mass discrimination in the analytical quadrupole mass spectrometer (M_r) to be assessed. To achieve the former with regard to trace gas analysis using SIFT-MS, we must also resort to simple diffusion theory. Finally, we discuss the overall influence of diffusion enhancement and mass discrimination in the quantification of trace gases using SIFT-MS.

Experimental Procedures

TSIFT Experiments

The experiments described in this paper were carried out using the TSIFT apparatus (manufactured to our design by Europa Scientific Ltd., U.K, now trading as PDZ Europa Ltd, U.K). However, they act as a guide to the procedure for validating any SIFT-MS instrument, as we will emphasise in the last section of this paper. Precursor positive ions are generated in a microwave discharge through a water vapour/air mixture in the ion source shown schematically in Figure 1. In this way, adequate currents of H_3O^+, NO^+ and O_2^+ can be selected by the upstream (injection) mass filter and injected into the helium carrier gas via the ion injection orifice shown in the inset. For the present studies we used H_3O^+ precursor ions exclusively as we will explain below. The ions are entrained in the carrier gas and convected along the flow tube and sampled downstream by an ion sampling orifice (area a) located at the center of the downstream sampling disc (area A) as are shown in Figure 1. This sampling disc is electrically isolated, which allows the ion current that is convected to it, I_d (typically 10 to 100 pA), to be measured. This allows an estimate of the ion current that can pass through the sampling orifice ($I_0 \sim I_d a/A$). The sampled ions are then focused into the analytical quadrupole mass spectrometer where they are mass analyzed and detected by the channeltron multiplier shown in Figure 1. Clearly, the ion current to the sampling disc can then be related to the ion count rate as determined by the channeltron detector. This is the critical aspect of this work. Such measurements allow the separate contributions of diffusive current enhancement of heavy ions (point 1 above) and mass discrimination against heavy ions (point 2 above) to be assessed.

Preparation of the Product Ions

A steady current of H_3O^+ ions was injected into the helium carrier gas thus creating a swarm of these precursor ions that is convected downstream by the helium. Thus, the current of H_3O^+ ions flowing into the sampling disc is measured and the count rate of these ions is recorded after selection by the mass spectrometer configured in a chosen way (see below). The major objective was then to rapidly convert the H_3O^+ ions to an appropriate single ionic species and to repeat the disc current and ion count rate measurements. To assist in this, we draw on the data obtained from our many SIFT studies of ion-molecule reactions [19–28] carried out in support of SIFT-MS. Thus, we chose to use the three aromatic hydrocarbons benzene (molecular weight 78 daltons), toluene (92 daltons) and m-xylene (106 daltons), all of which react with H_3O^+ by simple proton transfer [25] as, for example, benzene:

$$H_3O^+ + C_6H_6 \rightarrow C_6H_7^+ + H_2O \quad (2)$$

A further reason for the choice of these compounds as reactant gases, M, is that the product MH^+ ions do not react with their parent molecules at significant rates and thus they are effectively the terminating ions. So sufficient amounts of M can be flowed into the helium to ensure total conversion of the H_3O^+ ions to MH^+ ions at a position very close to the sample entry port (Figure 1). This then clearly defines the time period, t_r, over which these MH^+ ions can be lost to the flow tube walls by diffusion (eq 6). The hydrocarbons were introduced into the H_3O^+ ion/carrier gas swarm as a weak mixture of their vapor in dry cylinder air. Using these aromatic hydrocarbons, the H_3O^+ ions at $m/z = 19$ can be totally converted to ions at m/z of 79, 93 and 107. The changes in the convected ion currents to the sampling disc and the ion count rates can now be recorded for H_3O^+ ions only, and then for MH^+ ions only for particular settings of the quadrupole mass spectrometer. As we will show later, it was immediately apparent that mass discrimination (described by the M_r value) is dependent on the resolution setting of the analytical quadrupole mass spectrometer and to some extent on the energy of the ions in the analysing field, E_i. So in these experiments the M_r values were determined for several values of both the resolution setting and E_i.

To extend the range of m/z we also utilized the reactions of H_3O^+ ions with three ketones, acetone (58 daltons), 2-butanone (72 daltons) and 3-pentanone (86 daltons). We know from a previous study [19] that ketones react with H_3O^+ ions by proton transfer only, e.g., for acetone:

$$H_3O^+ + CH_3COCH_3 \rightarrow CH_3COCH_3H^+ + H_2O \quad (3)$$

Further, we know that secondary reaction of the protonated ketones, MH^+, with their parent molecule, M, finally ends with the formation of the proton-bound dimer ions, MH^+M, e.g.:

$$H_3O^+ + 2CH_3COCH_3$$
$$\rightarrow CH_3COCH_3H^+CH_3COCH_3 + H_2O \quad (4)$$

Thus, by adding sufficient ketone to the helium carrier gas the H_3O^+ precursor ions can be totally converted to MH^+M dimer ions. Thus, for acetone, *m/z* is increased from 19 (precursor ions) to 117 (product ions). Similarly, the other proton-bound ketone dimer ions can be formed. In this way, ions at *m/z* values of 117, 145 and 173 are created. So, in total, six product (investigator) ions were used with *m/z* values of 79, 93, 107, 117, 145 and 173.

Sample mass spectra are shown in Figure 2 together with the respective measured ion count rates. Also indicated are the respective sampling disc ion currents, I_d. To calculate M_r, the count rates of the ^{13}C isotopic variant ions were added to the count rates of the major product ions. The I_d values are plotted against *m/z* for the MH^+ and MH^+M ions in Figure 3 for a fixed injected current of H_3O^+ precursor ions. From such ion current and count rate measurements, mass discrimination in the analytical mass spectrometer can be quantified from the ratios of the disc currents and the ion count rates, and the phenomenon of diffusion enhancement can be explored from the fractional increase of the disc current.

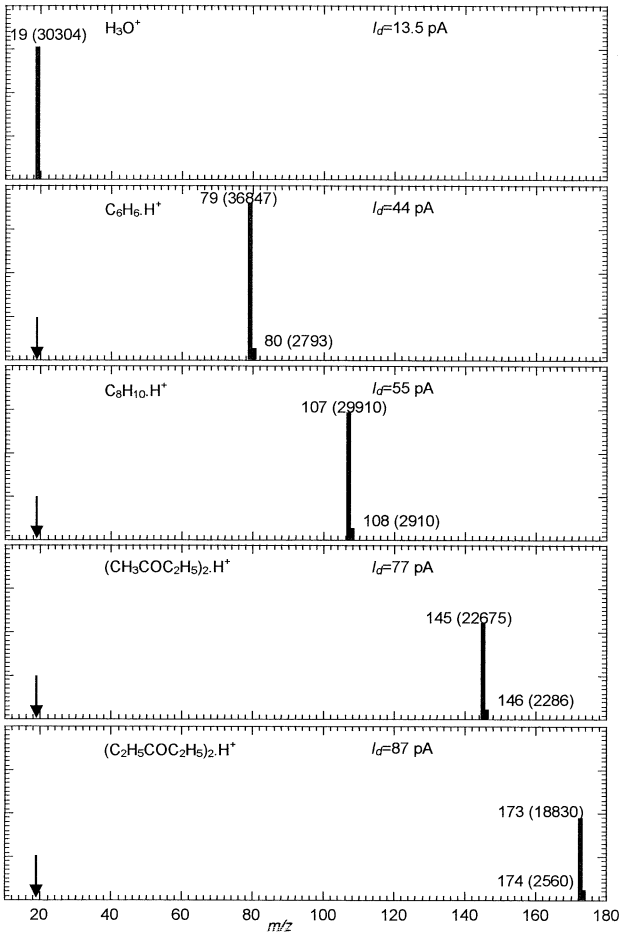

Figure 2. Mass spectra obtained using the downstream analytical quadrupole mass spectrometer. The value of *m/z* is shown for each detected ion signal together with the recorded signal intensity given in brackets in counts per second (c/s). The ion current, I_d, in picoamps (pA) collected by the downstream sampling disc is given for each mass spectrum. The first mass spectrum labeled H_3O^+ was obtained when the H_3O^+ precursor ions were injected in the absence of any reactant vapour. The next two mass spectra ($C_6H_6{\cdot}H^+$ and $C_8H_{10}{\cdot}H^+$) correspond to full conversion of the H_3O^+ precursor ions (*m/z* value of 19 as indicated by the arrows) to the protonated hydrocarbon close to the sample entry port. The last two mass spectra $(CH_3COC_2H_5)_2{\cdot}H^+$ and $(C_2H_5COC_2H_5)_2{\cdot}H^+$ show the full conversion of the H_3O^+ precursor ions to proton-bound dimer ions of two ketones. The injected current of the precursor ions is constant for all spectra shown here. The energy of the ions passing through the downstream quadrupole, E_i, was fixed at 7 eV and the resolution was also fixed at a setting corresponding to a FWHM of the ion peaks of 1.1 at an *m/z* = 173.

Results

Diffusion Enhancement

The effect of diffusion enhancement can immediately be observed in the simple experiments described above. When the H_3O^+ ions are totally converted to the heavier MH^+ or MH^+M product ions in reaction with the reactant gas M, there are very obvious increases in the ion current, I_d, collected to the downstream sampling disc as can be seen in Figure 3.

Unfortunately, such simple sampling disc current measurements cannot be directly used to determine the magnitude of diffusion enhancement during actual SIFT-MS analyses, because, for these analyses, the essential requirement is that only a small fraction of the precursor ions (a few percent maximum) should be converted to product ions. Under such circumstances, the ionic current to the sampling disc is due almost entirely to the flow of precursor ions and does not change appreciably because of the presence of trace gases in the sample to be analyzed. Further, it is clear that the analysis of complex gas samples (such as breath) leads to the formation of several MH^+ product ions with *m/z* values varying over a wide range, each with different diffusion rates in the helium carrier gas. These MH^+ product ions are formed along the whole length of the reaction zone (Figure 1) by the ion-molecules reactions and simultaneously lost to the flow tube walls by diffusion. To treat this complex situation and to obtain values for the diffusion enhancement for each product ion under trace gas analysis conditions, we have to resort to a theoretical analysis which involves the loss of precursor (H_3O^+) ions and the pro-

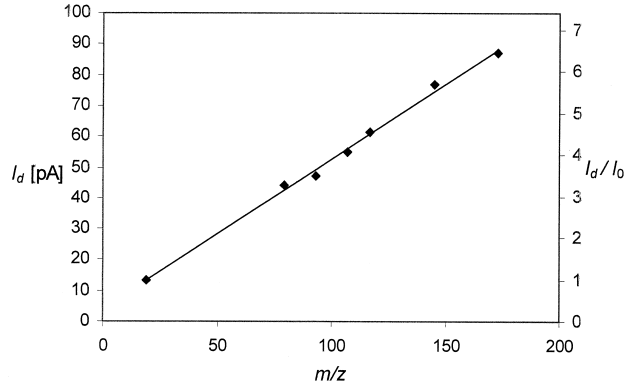

Figure 3. The downstream sampling disc ion current, I_d, in picoamps (pA) plotted against *m/z* for the H_3O^+, $C_6H_6{\cdot}H^+$, $C_7H_8{\cdot}H^+$, $C_8H_{10}{\cdot}H^+$, $(CH_3COCH_3)_2{\cdot}H^+$, $(CH_3COC_2H_5)_2{\cdot}H^+$, and $(C_2H_5COC_2H_5)_2{\cdot}H^+$ ions. A fixed current of H_3O^+ precursor ions was injected into the He carrier gas at a pressure of 0.7 torr and temperature of 300 K. Conversion of the precursor ions to the product ions occurred close to the sample entry port. The right axis shows the values of the ratio of I_d to the downstream sampling disc ion current of H_3O^+ in the absence of the reactant I_0 = 13.5 pA. Note that these currents do not depend on the settings of the downstream mass spectrometer.

duction and loss of product (MH^+) ions. Furthermore, we need to know the appropriate diffusion coefficients for H_3O^+ ions and those product ions involved in each particular SIFT-MS analysis. We can obtain a guide to the required diffusion coefficients from previously published work, and essential corroborative data can be derived from the disc current measurements described above under the identical conditions of SIFT-MS analyses.

It is fortunate that the phenomenon of ionic diffusion in gases has been researched for decades, notably by McDaniel and colleagues [33], and so a very useful database of the mobilities of ions in helium exists which can be called upon [34]. In the light of these previous data, the general trend of increasing I_t with *m/z* shown in Figure 3 is to be expected, because the pressure-dependent free-diffusion coefficients, D_p, of the different ions in the helium carrier gas, which are related to the ion mobility, K_0, via the Einstein relation [33], decrease with increasing *m/z* [35]. K_0 depends in detail on the interaction potential of the ions on the helium atoms [33] and does not decrease with increasing mass in a simple, predetermined way, although a simple correlation has been theoretically described for a range of protonated amines [36]. Langevin theory [33] indicates a simple dependence of mobility on *m/z* for small ions [35]. For large ions, the geometry of the ion [37, 38] and the details of the interaction potential can have a significant influence [36].

Theoretical analysis of the sampling disc current for full ionic conversion. First we consider diffusion in the TSIFT in the absence of reactant gas. The H_3O^+ precursor ions are lost from the flow tube by diffusion to the walls where they are neutralized on the surface. This results in the establishment of a fundamental mode diffusion distribution upstream of the sample inlet. The ion density is then at a maximum value on the axis of the flow tube [18]. Simple diffusion theory within a long cylindrical tube now indicates that the axial (time) variation of the H_3O^+ ion number density, $[H_3O^+]$, is given by:

$$[H_3O^+]_t = [H_3O^+]_0 \exp\left(-\frac{D_p(H_3O^+)}{\Lambda^2}\, t\right) \qquad (5)$$

$[H_3O^+]_0$ is the number density of the H_3O^+ ions at the sample entry port, Λ is the characteristic diffusion length of the flow tube determined from only its dimensions [33] and t is the diffusion time as an independent variable. The zero-field reduced mobility, K_0, of H_3O^+ ions in helium at 300K is 21.5 $cm^2V^{-1}s^{-1}$ [39]. This is equivalent to a free diffusion coefficient, $D_p(H_3O^+)$, for these ions of 434 cm^2s^{-1} at 1 torr (corresponding to a value of 620 cm^2s^{-1}at pressure of 0.7 torr which we used in these experiments, and which is commonly used for SIFT-MS [2]). The flow tube diameter is 4.1 cm and thus Λ = 0.83 cm [33].

When a sufficiently large flow of, for example, hydrocarbon vapor is introduced into the helium, proton transfer occurs from the H_3O^+ ions to the hydrocarbon molecules, M (eq 5). For a very large number density [M], all the H_3O^+ ions are immediately converted to MH^+ ions at the sample entry port. Then an equation analogous to eq 5 indicates the time variation of the number density of MH^+ ions as:

$$[MH^+]_t = [H_3O^+]_0 \exp\left(-\frac{D_p(MH^+)}{\Lambda^2}\, t\right) \qquad (6)$$

The MH^+ ion current, I_d, and the H_3O^+ ion current, I_0, measured at the sampling disc are proportional to the MH^+ and H_3O^+ ion number densities respectively at the downstream sampling disc. These number densities can be calculated from the known residence time of the ions in the reaction zone t_r. that is between the sample entry port and the downstream sampling disc (Figure 1). t_r is 3.4 ms in the TSIFT instrument under consideration. It therefore follows from eq 5 and 6 that the current enhancement, when all the H_3O^+ ions are converted rapidly to MH^+ ions is:

$$I_d/I_0 = \exp\left(\frac{D_p(H_3O^+) - D_p(MH^+)}{\Lambda^2}\, t_r\right) \qquad (7)$$

Thus, the current enhancement is a measure of $D_p(MH^+)$ (since t_r and Λ are known). Although the data in Figure 3 do not relate to SIFT-MS analyses directly, they now allow the D_p for the MH^+ and MH^+M product ions to be determined using eq 7. The values of diffusion coefficients thus obtained characterize diffusion of the MH^+ ions through a mixture of helium

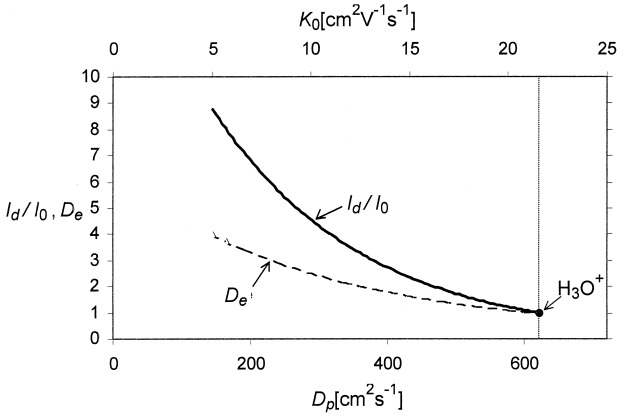

Figure 4. Results of theoretical calculations. The full line shows the relationship between the current enhancement, I_d/I_0, when all the H_3O^+ ions are converted rapidly to the product ions and the product ion diffusion coefficients, D_p, according to eq 7. The top abscissa shows the values of reduced zero field ion mobilities, K_0, corresponding to those D_p values at a pressure of 0.7 torr indicated on the bottom abscissa. The H_3O^+ precursor ion diffusion coefficient is taken as 620 cm^2s^{-1} corresponding to a K_0 of 21.5 $cm^2V^{-1}s^{-1}$ (indicated by the vertical dotted line). The dashed line is the dimensionless diffusion enhancement coefficient, D_e, for product ions appropriate to trace gas analysis conditions as a function of D_p (under identical conditions) calculated using eq 10.

(>98%) and air (<2%) with small amounts of water (<0.03%) and the reagent vapor (<0.005%). Thus, according to Blanc's law [33], the measured values of D_p will be somewhat lower than those appropriate to pure helium, but they are directly applicable to typical SIFT-MS conditions. It is most useful to plot $I_{MH^+}/I_{H_3O^+}$ against the reduced mobilities, K_0, which are simply derived from the D_p values (again using the Einstein relation [33], and such a plot is given in Figure 4 for the particular SIFT-MS instrument under consideration. Note that for H_3O^+ ions (K_0 = 21.5 $cm^2V^{-1}s^{-1}$) the current ratio is chosen as unity. The derived K_0 values for the various MH^+ and MH^+M ions are listed in Table 1. These reduced mobilities are consistent with the few

Table 1. Zero-field reduced mobilities, K_0, and the dimensionless diffusion enhancement coefficients, D_e, derived from the downstream sampling disc current measurements

Ion	m/z	K_0 ($cm^2V^{-1}s^{-1}$)	D_e
H_3O^+	19	21.5[a]	1.0
$C_6H_6.H^+$	79	12.8[b]	2.0[c]
$C_7H_8.H^+$	93	12.3	2.1
$C_8H_{10}.H^+$	107	11.1	2.3
$(CH_3COCH_3)_2.H^+$	117	10.6	2.4
$(CH_3COC_2H_5)_2.H^+$	145	7.2	3.2
$(C_2H_5COC_2H_5)_2.H^+$	173	5.7	3.7

[a] The value of K_0 for H_3O^+ is taken from [39] and serves as a reference for the other K_0 values derived in this study.
[b] The value measured in a drift tube [40] for $C_6H_6.H^+$ is 11.6 $cm^2V^{-1}s^{-1}$. The uncertainty in our K_0 values is estimated to be ± 2 $cm^2V^{-1}s^{-1}$.
[c] The D_e values were obtained for helium at a pressure of 0.700 torr containing 2% of air, a temperature of 300 K, a flow tube diameter of 4.1 cm and a diffusion time of 3.4 ms.

published values for relatively large organic ions in pure helium [40]; for $C_6H_7^+$ ions K_0 =11.6 $cm^2V^{-1}s^{-1}$; for $C_{10}H_8^+$ ions K_0 = 8.8 $cm^2V^{-1}s^{-1}$).

Theoretical analysis of D_e for trace gas analysis. Now we consider the more complex situation of SIFT-MS analysis when diffusion of the precursor H_3O^+ ions occurs continuously with some small loss (not more than a few percent) via reactions with trace gas molecules, M, continuously producing MH^+ ions. The only two ion species in the carrier gas are H_3O^+ and MH^+ ions. The time variations of $[H_3O^+]$ is given by:

$$[H_3O^+]_t = [H_3O^+]_0 \exp\left(- k[M]t - \frac{D_p(H_3O^+)}{\Lambda^2} t \right) \quad (8)$$

k is the rate coefficient for the reaction of the H_3O^+ ions with the trace gas molecules present at a number density [M]. The continuously formed MH^+ ions are also partly lost by diffusion, but their residence time in the flow tube is now not fixed at t_r as for the previous scenario described by eq 6, but it varies from t_r down to zero. The analytical solution of the set of ordinary differential equations describing this complex situation [2] gives the time variation of the MH^+ number density, $[MH^+]$, as:

$$[MH^+]_t = [H_3O^+]_t k[M]t \cdot \frac{\exp\left(k[M]t + \frac{D_p(H_3O^+) - D_p(MH^+)}{\Lambda^2} t \right) - 1}{k[M]t + \frac{D_p(H_3O^+) - D_p(MH^+)}{\Lambda^2} t} \quad (9)$$

The effect of differential diffusion is now described by the large fraction term in eq 9, which for $t = t_r$ can be represented by a diffusion enhancement coefficient, D_e. In the limit of [M] = 0 (applicable to trace gas analysis by SIFT-MS):

$$D_e = \lim_{[M]\to 0} \frac{[MH^+]_{tr}}{[H_3O^+]_{tr} k[M] t_r} = \frac{\exp\left(\frac{D_p(H_3O^+) - D_p(MH^+)}{\Lambda^2} t_r \right) - 1}{\frac{D_p(H_3O^+) - D_p(MH^+)}{\Lambda^2} t_r} \quad (10)$$

This expression for D_e clearly converges to 1 for $D_p(H_3O^+) = D_p(MH^+)$, i.e., when the diffusion losses are identical. This is indicated in Figure 4 where eq 10 is graphically represented as a plot of the calculated D_e against D_p (and the corresponding K_0) for the conditions of these experiments. The values of D_e calculated for the six ionic species included in this study are given in Table 1 and they are plotted against m/z in Figure 5.

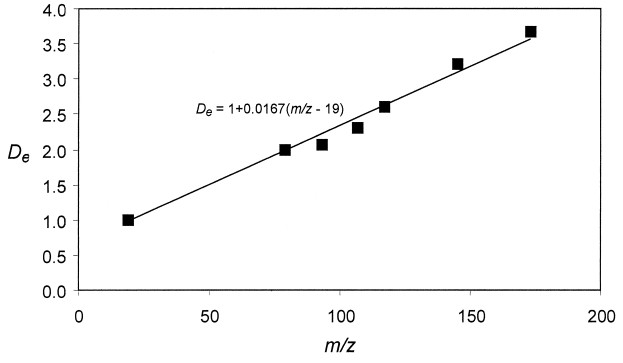

Figure 5. Values of the dimensionless diffusion enhancement coefficient, D_e, obtained from the I_d/I_0 data given in Figure 3 plotted against the *m/z* values of the product ions. There is an excellent linear correlation between D_e *and m/z* for these product ions as is described by the equation given in the figure (the coefficient of determination, R^2, is 0.98).

Note that there is an acceptably linear correlation between D_e and *m/z* for the ions included in this study. This is a reflection of the correlation of the ion mobilities with *m/z* for these polyatomic organic ions. Note also that these values of D_e refer to the particular circumstances of the TSIFT instrument used for these experiments.

Mass Discrimination

With a good understanding of diffusion enhancement in these flow tube systems and its effect on the currents of particular ions arriving at the sampling orifice, we can now proceed to discuss mass discrimination in the analytical quadrupole mass spectrometer.

The basic assumption made in this study is that the current of a particular ionic species arriving at the mass spectrometer sampling disc, I_d, is proportional to the flux of that ionic species through the sampling orifice, I_0. By relating I_0, or simply $I_d = I_0 A/a$; (see previous) to the count rate of those ions, C_i, at the channeltron detector (including all isotopic variants), a mass discrimination factor, M_r, can be defined as I_d/C_i for this particular ionic species. The M_r value will refer to a specific set-up of the mass spectrometer, the resolution, and to a lesser extent the energy of the ions in the analyzing field, E_i; are of prime importance. At the beginning of this discussion, we repeat that the M_r for a particular ionic species may, in part, be dependent on its efficiency of transmission through the sampling orifice and its detection efficiency by the channeltron detector. Both these efficiencies may be different for ions of different mass, but we have no real evidence that either of these possible effects is significant.

Again, it makes sense to normalize the M_r values to that for the lowest mass precursor ions under consideration for SIFT-MS, i.e., the H_3O^+ ions. Hence, we set $M_r(H_3O^+) = 1$ and (see below) the M_r values for all ions of greater *m/z* are equal to or greater than one. This does not imply that the absolute transmission coefficient for H_3O^+ ions is unity. However, it is desirable that the transmission of the precursor ions used in SIFT-MS is close to unity to optimise the counting statistics and thus to improve the precision of this analytical instrument. Optimal transmission is achieved by suitable choice of the ΔM parameter and of the resolution in these quadrupole mass filters, which are dependent on the relative amplitudes of the rf and dc voltages on the quadrupole rods [41]. An estimate of the transmission efficiency for the H_3O^+ ions can be made from the values of I_o and the count rates of the H_3O^+ ions. Thus, for a typical value of $I_0(H_3O^+)$ in these experiments of 15 pA and since a/A is 2.3×10^{-4} (derived from the dimensions given in Figure 1), the expected ion count rate for 100% transmission through the quadrupole mass spectrometer is about 2×10^4/s. The corresponding experimentally determined count rate of the ions is typically 3×10^4/s, which is actually larger than the simple calculation predicts. This is most probably because for fundamental mode diffusion, the number density of ions on the axis of the flow tube (where the sampling orifice is located) is greater than the mean ion density across the sampling disc which actually constitutes the ionic current to the disc. However, this simple estimate shows that for this ion sampling/mass spectrometer/detection system, the transmission efficiency for these lower mass ions is actually close to unity.

The data obtained from this TSIFT instrument reveal that there is a quadratic relationship between M_r and *m/z* over the *m/z* range from 19 to 173:

$$M_r(m/z) = 1 + f_2(m/z - 19)^2 \quad (11)$$

The coefficient f_2 can be obtained from a least squares fit through multiple data points of the normalized C_i/I_d ratio for each setting of the resolution and of E_i. The standard deviation of the residuals of M_r (the differences between the data and the fit) is less than 0.5. Higher-order polynomials or a different functional form might be required for *m/z* values above 200 or for a different quadrupole mass spectrometer.

The derived M_r values for the several ions included in this study obtained for three values of E_i at a fixed resolution of the mass spectrometer are shown in Figure 6. The M_r values obtained for three resolutions at a fixed value of E_i equal to 7 electron volts (eV) which is typically used for quadrupole mass filters, are shown in Figure 7. For the purpose of this work we describe the resolution of the mass spectrometer as the full width at half maximum (FWHM), ΔM, of the mass peaks. Note how peak splitting occurs for low resolution (ΔM above 1) for this quadrupole mass spectrometer. The data in these figures show that M_r at first increases relatively slowly with *m/z*, reaching a value of about 2.2 at an $m/z = 79$ (the protonated benzene molecule) for an E_i of 7 eV at the lowest resolution investigated in these experiments. At *m/z* values above about 100, M_r in-

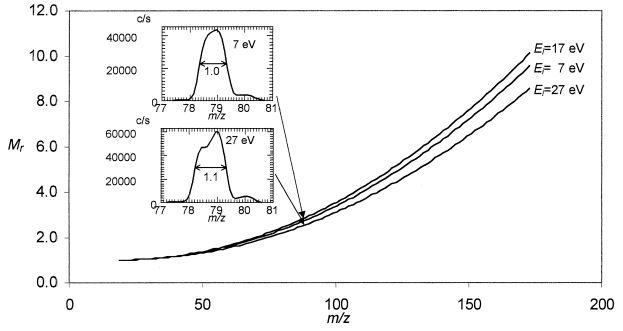

Figure 6. Curves characterizing the degree of mass discrimination of the downstream mass spectrometer, i.e., M_r as a function of m/z according to eq 11, obtained from the measured values of the downstream disc currents and the ion count rates using a least squares fitting procedure, for three values of ion energy, E_i, in the quadrupole. The insets show peak shapes for the product ion (protonated benzene at m/z 79 was chosen as the lightest product ion for this study) for the lowest (7 eV) and the highest (27 eV) values of E_i investigated. The FWHM indicated by the horizontal arrows increase from 1.0 to 1.1 even though the resolution setting was kept at a fixed value.

creases more rapidly, reaching a value of about 9 near m/z = 173. The plots shown in Figure 6 show that M_r is not greatly dependent on E_i but the plots shown in Figure 7 show a more seriously dependence of M_r on the resolution of the mass spectrometer, as is the case for all mass spectrometers. Of course, it is imperative for SIFT-MS analyses that the analytical mass spectrometer is operated at sufficiently high resolution to result in the clear separation of product ions with adjacent m/z values. It is necessary to settle for rather large M_r values at the higher m/z values around 170 to 180, as can be seen in Figure 7, where typical mass spectra around m/z of 173 are shown for three different resolutions at which the M_r values are near 9, 10 and 12.

So the values of M_r are large at the larger m/z, which

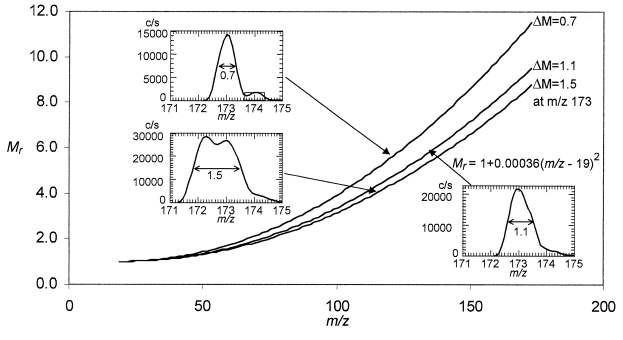

Figure 7. The dependencies of M_r on m/z following the same procedure as for Figure 6 but this time for three different resolution settings of the downstream quadrupole mass spectrometer at a fixed value of E_i of 7 eV. The insets show the peak shapes of the product ion (the proton-bound dimer ion of pentanone at m/z = 173 was chosen as the heaviest product ion included in this study). The FWHM of these peaks are 0.7, 1.1 and 1.5 as indicated by the horizontal arrows for the three different resolution settings. The dependence of M_r on m/z for the optimum intermediate resolution 1.1 setting is described by the equation shown in the figure. Note the severe peak splitting at the lowest resolution.

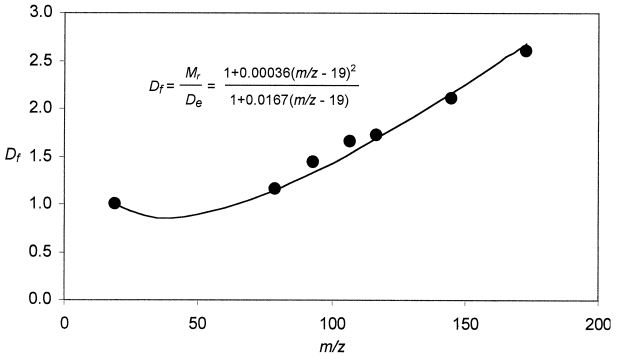

Figure 8. The values of the overall SIFT-MS discrimination factor, $D_f = M_r/D_e$ for the optimal setting of the downstream mass spectrometer and for a FWHM resolution of 1.1 at m/z = 173 and an E_i = 7 eV. The data points are the experimentally derived values for the ions included in this study. The line indicates the variation obtained using the expression shown in the figure, which was obtained from the expressions given in Figures 5 and 7.

means severe mass discrimination. If unaccounted for, this would result in unacceptably large errors in SIFT-MS analyses involving product ions with m/z values above 100. We have determined the M_r values for two other SIFT-MS instruments (another TSIFT and our larger laboratory SIFT) and obtained similar results to the above. It is clear, therefore, that the above exercise is required for any quadrupole mass spectrometer that is to be used for quantitative analysis.

Relevance to Quantitative Analysis by SIFT-MS

As noted before, diffusion enhancement represented by D_e and mass discrimination represented by M_r are counteracting phenomena, M_r acting to lower the detected product ion count rates and D_e enhancing these. It is therefore useful for analysis to define an overall SIFT-MS discrimination factor, $D_f = M_r/D_e$, which is a measure of the net influence of these two effects. The D_f values derived from the D_e and M_r data for this particular TSIFT instrument are plotted against m/z in Figure 8. it can be seen for ions with m/z values below 60 that the predicted D_f is somewhat less than unity because diffusion enhancement has a greater effect than mass discrimination within this range. The D_f value increases to 1.15 at m/z = 79 ($C_6H_6H^+$ ions). Thus the two opposing factors essentially cancel each other out within ±15% in the range of m/z from 19 to 79. At an m/z of about 100, D_f has a value near to 1.4, which shows that quantification of trace gases that lead to such product ions would be erroneously low (by about 40%) if these effects were not taken into account. For product ions with m/z values close to 173, D_f reaches a value of 2.6 and thus an equivalent error in analysis would be introduced if this factor were ignored. However, the all-important point is that D_f can now be included into the SIFT-MS analytical procedure in the form shown in

Figure 8, thus improving the quantification of trace gases accordingly.

Conclusion

This study has shown how important it is to account for ionic diffusion enhancement (D_e) in the flow tube and mass discrimination in the analytical quadrupole mass spectrometer (M_r) to accurately quantify trace gases in air/breath mixtures by SIFT-MS using our TSIFT. For the larger laboratory SIFT, both D_e and M_r, and hence D_f, are relatively small, explaining why the validation of this as a SIFT-MS analytical instrument was so persuasive [12, 13]. These observations serve to emphasise the point that all SIFT-MS instruments may differ, certainly for differing quadrupole configurations, and the influences of diffusion enhancement and mass discrimination must be considered for each instrument according to the experiments described in this paper. It is now a routine procedure in the SIFT-MS instruments used for applied research, that a D_f correction is an integral part of the analytical software.

Acknowledgments

Thr authors gratefully acknowledge financial support by the Grant Agency of the Czech Republic, Project number 203/00/0632, and the Engineering and Physical Sciences Research Council, U.K., grant reference GR/M89195/01. They also thank the Royal Society of London for the award of a Joint Project Grant that supports the essential collaboration between the authors. Finally, they are very grateful to Ann Diskin for her help in the acquisition of the experimental data.

References

1. Španěl, P.; Smith, D. *Int. Rev. Phys. Chem.* **1996,** *15*, 231–271.
2. Španěl, P.; Smith, D. *Med. Biol. Eng. Comput.* **1996,** *34*, 409–419.
3. Smith, D.; Španěl, P. In *Encyclopedia of Spectroscopy and Spectrometry, Mass Spectrometry,* Lindon, J.; Trantner, G.; Holmes, J. Eds.; Academic Press; London, 1999; pp. 2092–2105.
4. Španěl, P.; Smith, D. *Rapid Communications in Mass Spectrometry* **1999,** *13*, 585–597.
5. Španěl, P., Smith, D.; Holland, T. A.; Al Singary, W.; Elder, J. B. *Rapid Communications in Mass Spectrometry* **1999,** *13*, 1354–1359.
6. Harrison, A. G. *Chemical Ionisation Mass Spectrometry, 2nd ed.*; CRC Press: Boca Raton, Florida, 1992.
7. Manolis, A. *Clinical Chemistry* **1983,** *29*, 5–15.
8. Davies, S.; Španěl, P.; Smith, D. *Kidney International* **1997,** *52*, 223–228.
9. Smith, D.; Španěl, P.; Davies, S. *Journal of Applied Physiology* **1999,** *87*, 1584–1588.
10. Smith, D.; Španěl, P.; Jones, J. B. *Bioresources Science and Technology* **2000,** *75*, 27–33.
11. Španěl, P.; Smith, D. *Rapid Communications in Mass Spectrometry* **2000,** *14*, 1136–1140.
12. Španěl, P.; Cocker, J.; Rajan, B.; Smith, D. *Ann. Occup. Hyg.* **1997,** *41*, 373–382.
13. Smith, D.; Španěl, P.; Thompson, J. M.; Rajan, B.; Cocker, J.; Rolfe, P. *Applied Occupational and Environmental Hygiene* **1998,** *13*, 817–823.
14. Španěl, P.; Smith, D. *Rapid Communications in Mass Spectrometry* **2000,** *14*, 1898–1906.
15. Arnold, F.; Knop, G. *Int. J. Mass Spectrom. Ion Proc.* **1987,** *81*, 33–44.
16. Arijs, E.; Barassin, A.; Kopp, E., Amelynck, C.; Catoire, V.; Fink, H. P.; Guimbaud, C.; Jenzer, U.; Labonnette, D.; Luithardt, W.; Neefs, E.; Nevejans, D.; Schoon, N.; Van Bavel, A. M. *Int. J. Mass Spectrom.* **1998,** *181*, 99–111.
17. De Gouw, J. A.; Howard, C. J.; Custer, T. G; Baker, B. M.; Fall, R. *Environmental Science and Technology* **2000,** 34, 2640–2648.
18. Smith, D.; Adams, N. G. *Advances in Atomic and Molecular Physics* **1988,** *24*, 1–49.
19. Španěl, P.; Yufeng, Ji; Smith, D. *Int. J. Mass Spectrom. Ion Processes* **1997,** *165/166*, 25–37.
20. Španěl, P.; Smith, D. *Int. J. Mass Spectrom.* **1997,** *167/168*, 375–388.
21. Španěl, P.; Smith, D. *Int. J. Mass Spectrom.* **1998,** *172*, 137–147.
22. Španěl, P.; Smith, D. *Int. J. Mass Spectrom.* **1998,** *172*, 239–247.
23. Španěl, P.; Smith, D. *Int. J. Mass Spectrom.* **1998,** *176*, 203–211.
24. Španěl, P.; Smith, D. *Int. J. Mass Spectrom.* **1998,** *176*, 167–176.
25. Španěl, P.; Smith, D. *Int. J. Mass Spectrom.* **1998,** *181*, 1–10.
26. Španěl, P.; Smith, D. *Int. J. Mass Spectrom.* **1999,** *184*, 175–181.
27. Španěl, P.; Smith, D. *Int. J. Mass Spectrom.* **1999,** *185/186/187*, 139–147.
28. Španěl, P.; Smith, D. *Int. J. Mass Spectrom.* **1999,** *189*, 213–223.
29. Smith, D.; Španěl, P. *Mass Spectrometry Reviews* **1995,** *14*, 255–278.
30. *Generation of test atmospheres of organic vapours by the syringe injection technique, MDHS 3, Methods for the Determination of Hazardous Substances*. Health and Safety Executive: London, 1990.
31. Dawson, P. H.; Whetten, N. R. *Adv. Electronics Electron Phys.* **1969,** *39*, 60–185.
32. Španěl, P.; Davies, S.; Smith, D. *Rapid Communications in Mass Spectrometry* **1999,** *13*, 1733–1738.
33. Mason, E. A.; McDaniel, E. W. *Transport Properties of Ions in Gases*; Wiley Interscience: New York, 1988.
34. Ellis, H. W.; Pai, R. Y.; McDaniel, E. W.; Mason, E. A.; Viehland, L. A. *At. Data. Nucl. Tables* **1976,** *17*, 177–210.
35. Lindinger, W.; Albritton, D. L. *J. Chem. Phys.* **1975,** *62*, 3517–3522.
36. Berant, Z.; Karpas, Z. *J. Am. Chem. Soc* **1989,** *111*, 3819–3824.
31. vonHelden, G.; Hsu, M. T.; Gotts, N.; Bowers, M. T. J. *Phys. Chem.* **1993,** *97*, 8182–8192.
38. deGouw, J. A.; Krishnamurthy, M.; Bierbaum, V. M.; Leone, S. R. *Int. J. Mass Spec.* **1997,** *167*, 281–289.
39. Ellis, H. W.; McDaniel, E. W.; Albritton, D. L.; Viehland, L. A.; Lin, S. L; Mason, E. A. *At. Data. Nucl. Tables* **1978,** *22*, 179–217.
40. Krishnamurthy, M.; deGouw, J. A.; Bierbaum, V. M.; Leone, S. R. *J. Chem. Phys.* **1996,** *100*, 14908–14913.
41. Paul, W.; Reinhard, H. P.; von Zahn, U. Z. *Phys.* **1958,** *152*, 143–182.